

Surface phonons and dipole activity of Si(111)2×1 from *ab initio* calculations

F. Ancilotto

*International School for Advanced Studies, 34014 Trieste, Italy
and Dipartimento di Fisica, Università di Padova, 35100 Padova, Italy*

A. Selloni

International School for Advanced Studies, 34014 Trieste, Italy

W. Andreoni

IBM-Zurich Research Laboratory, CH-8803 Rüschlikon, Switzerland

S. Baroni and R. Car

International School for Advanced Studies, 34014 Trieste, Italy

M. Parrinello

*International School for Advanced Studies, 34014 Trieste, Italy
and IBM-Zurich Research Laboratory, CH-8803 Rüschlikon, Switzerland*

(Received 8 November 1990)

We present a first-principles linear-response study of the phonon spectrum and dipole activity of the Si(111)2×1 surface. Our results are in good agreement with the experimental He-scattering results for the acoustic modes, as well as the electron-energy-loss data for the optical modes. We clarify a current controversy on the assignment of the electron-energy-loss peak at ~ 56 meV. We find that the dominant contribution to the loss peak is anisotropic and arises from a longitudinal-optical vibration of the surface chains. However, a small but non-negligible isotropic contribution comes from subsurface modes polarized perpendicular to the surface.

Experimental observations of the static properties of the 2×1 reconstructed surface of silicon¹ appear to be well understood on the basis of Pandey's π -bonded chain model.² This model has recently obtained further theoretical support from *ab initio* molecular-dynamics³ simulations, which have yielded a π -bonded chain structure starting directly from the ideal (111) surface.⁴ Experimental data on the vibrational properties of Si(111)2×1, instead, are still the subject of some controversy. In fact, recent electron-energy-loss-spectroscopy (EELS) measurements^{5,6} in the optic region, although confirming the long-established existence of a strongly dipole-active mode at ~ 56 meV,⁷ have provided a controversial picture of the character of this mode. Theory has not been able to clarify this issue, since empirical tight-binding calculations attribute this mode to a longitudinal-optical vibration of the surface π -bonded chains,⁸ whereas bond-charge-model calculations assign it to a subsurface vibration polarized perpendicular to the surface.⁹ Other interesting features characterize the vibrational spectrum of Si(111)2×1. In particular, in the acoustic region, He-

scattering data have revealed, in addition to the usual Rayleigh wave, an almost dispersionless excitation at ~ 10 meV.¹⁰

In this paper, we present a detailed first-principles study of the phonon spectrum and dipole activity of Si(111)2×1, based on the density-functional linear-response-theory (DF-LRT) scheme of Ref. 11. In a previous publication, we presented results of an *ab initio* molecular-dynamics (MD) calculation of the structural, electronic, and vibrational properties of Si(111)2×1.⁴ This scheme produced very good results for the (equilibrium) $T = 0$ structure. Also the phonon spectrum that could be extracted from an analysis of the atomic trajectories was overall satisfactory, with the exception of two modes, which turned out to be anomalously soft. We will show here that this disagreement is not of a fundamental nature, and that the use of the DF-LRT scheme of Ref. 11 complements our previous MD results and leads to a remarkable agreement between theory and experiment. The results of the present study can be summarized as follows. In the optic region, we

find that the largest dipole activity is associated with longitudinal-optical vibrations of the surface chains at ~ 57 meV, which are strongly coupled to the surface π and π^* states at the zone edge of the surface Brillouin zone (SBZ), in agreement with the results of Refs. 5 and 8. We also find, however, a small but sizeable activity at energies $\sim 50 - 55$ meV from subsurface modes polarized perpendicular to the surface (*i.e.*, the modes that are the most active according to Ref. 9), thus providing support for the conclusions of Ref. 6, where both isotropic and anisotropic contributions to the EELS peak were found to occur. In the acoustic region of the spectrum, our results are consistent with the occurrence of an approximately flat branch at ~ 12 meV accompanying the Rayleigh wave, in agreement with He-scattering experiments.¹⁰

We recall here a few details of the MD calculations in Refs. 4 and 12. Repeated slabs of 64 Si atoms with a $(\sqrt{3} \times 4)$ surface cell (8 atoms/layer) were used. The lower surface was unreconstructed, with the dangling bonds saturated by a monolayer of hydrogen, and the vacuum region between slabs was ~ 9 Å wide. Only the electronic states at the Γ point of our MD supercell have been used. These have been expanded in plane waves (PW) with a kinetic-energy cutoff $E_{\text{cut}} = 8$ Ry. Due to our $(\sqrt{3} \times 4)$ surface supercell, three \mathbf{k} -points of the SBZ of the 2×1 unit cell fold into our Γ , namely $\bar{\Gamma}$, \bar{J} , and the point halfway between them. Six layers of Si atoms were allowed to move in all the calculations.

The equilibrium surface structure of our MD calculations was obtained using a simulated annealing technique, as explained in detail in Ref. 4. The resulting 2×1 Pandey-like geometry is characterized by a substantial buckling, $b \sim 0.49$ Å, of the topmost chain, in fairly good agreement with the experimental value $b = 0.38 \pm 0.08$ Å.¹³ The vibrational spectrum was obtained from the analysis of the equilibrium trajectories generated during a finite temperature MD run, as described in Ref. 12. Comparison of the layer-resolved phonon density of states (PDOS) with corresponding bulk results showed that the significant surface features were confined to the two top layers, thus justifying *a posteriori* our use of a thin slab to determine the surface phonon spectrum. In the optic region at $\bar{\Gamma}$ the most relevant surface features turned out to be two longitudinal-optical vibrations along the first- (D) and second- (D_2) layer chains at ~ 44 and ~ 60 meV, respectively, and two subsurface, yz -polarized modes at ~ 50 (I'') and ~ 55 meV (I') (we call x, y , and z the $[1\bar{1}0]$, *i.e.*, parallel to the chains, $[11\bar{2}]$, and $[111]$, *i.e.*, perpendicular to the surface directions, respectively). In the acoustic region we identified (i) at $\bar{\Gamma}$ several modes, among which two polarized mainly along z , at ~ 9 and ~ 12 meV, in agreement with He-scattering experiments where a broad resonance centered at ~ 10 meV is observed; (ii) at \bar{J} two prominent z -polarized modes, strongly localized on the surface chains: the Rayleigh wave (RW) at ~ 15 meV, *i.e.*, about 4 meV higher than the experiment,¹⁰ and a

mode (N_1) at ~ 5 meV, which, in spite of its anomalously low frequency, was assigned to the almost dispersionless excitation seen in He-scattering experiments at ~ 10 meV.¹⁰

In this MD calculation, the restricted \mathbf{k} -point sampling provided by the Γ point of our supercell may lead to possible inaccuracies in some properties. Also the methods used in Ref. 4 for extracting the phonon modes from the MD trajectories¹⁴ are able to accurately determine the eigenfrequencies, but provide only an approximate knowledge of the eigenvectors. For these reasons, we have calculated the dynamical matrix at the $\bar{\Gamma}$ and \bar{J} points of the SBZ using the DF-LRT scheme of Ref. 11. For the phonons at $\bar{\Gamma}$, the macroscopic dipole moment has also been calculated, using the approach described in Ref. 15. The technical details of these calculations are similar to the MD ones, but—in order to reduce the computational cost—repeated slabs of six (111) layers of Si and one layer of H are used. The equilibrium structure of the slab is the same as was used for the MD calculations. This structure has proved to be good not only in comparison with experiments, but also with regard to convergence with \mathbf{k} points, as discussed in Ref. 4. The only minor difference is that, due to the smaller number of layers used, we have taken the sixth-layer atoms to be in their ideal positions, while in Ref. 4 these were slightly displaced. Calculations using two different values of E_{cut} (6 and 8 Ry) and several different sets of \mathbf{k} points have been performed, in order to check the convergence with respect to E_{cut} and SBZ sampling. Moreover, since the number of layers is here reduced with respect to the MD calculations, we have studied the stability of the phonon modes relative to the change in boundary conditions, by performing calculations where the mass m_{H} of the H atoms on the lower surface was set equal either to its physical value or to infinity (this corresponds to fixing the position of the H atoms, as done in MD).

Our results, obtained with $E_{\text{cut}} = 8$ Ry and eight \mathbf{k} points in a direction parallel to $\bar{\Gamma}\bar{J}$, are given in Table I. Here we report only those modes that are not significantly affected by the change in m_{H} mentioned above (in particular, the results in the table refer to the case where m_{H} is equal to its physical value). In practice, this amounts to excluding only the lower-frequency part of the spectrum at $\bar{\Gamma}$, where the modes are strongly penetrating. However, even these modes do not change much with varying m_{H} , their frequencies being always confined in a band between ~ 9 and ~ 16 meV, in reasonable agreement with He-scattering experiments. All other modes at $\bar{\Gamma}$ and \bar{J} are instead very stable. Only slight changes occur in the eigenvectors, which give rise to changes of the order of 10% in the magnitude of the macroscopic dipole \mathbf{P} for the modes at $\bar{\Gamma}$.

The overall agreement between the DF-LRT and the MD results is quite good, the only noticeable exceptions being the frequencies of the D and N_1 modes: the frequencies obtained from DF-LRT are significantly higher, ~ 57 and ~ 12 meV, respectively. The softening of the D

TABLE I. Surface phonon spectrum at $\bar{\Gamma}$ and at the SBZ edge \bar{J} , obtained using DF-LRT (except for the column labeled E_{MD}), and taking the mass m_{H} of the H atoms on the lower surface equal to its physical value. Only the modes that are not affected by the slab boundary conditions are given (see text). We report energies (in meV) of the surface phonons (E); surface phonon energies obtained from MD (E_{MD}); degree of localization on the first (w_1), second (w_2), and third (w_3) layer; the main direction of polarization; the three components of the macroscopic dipole moment associated with the modes at $\bar{\Gamma}$. The letters in the left part of the Table label some modes that are discussed in the text.

	E	E_{MD}	w_1	w_2	w_3	Polarization	$ P_x $	$ P_y $	$ P_z $
$\bar{\Gamma}$									
R	19.6		0.66	0.07	0.02	z		1.09	0.05
I'''	47.7		0.29	0.25	0.15	yz		0.34	0.13
I''	49.8	(50.2)	0.30	0.52	0.04	yz		0.03	0.27
I'	55.8	(55.3)	0.03	0.25	0.54	yz		0.35	0.10
D	57.2	(44.0)	0.62	0.22	0.05	x	8.9		
D_2	60.8	(60.5)	0.23	0.42	0.03	x	5.7		
	65.4	(66.4)	0.50	0.45	0.01	y		0.74	0.12
	68.9 ^a		0.00	0.00	0.02	yz		0.12	0.01
\bar{J}									
N_1	11.8	(5.5)	0.80	0.09	0.01	z			
RW	17.4	(15.6)	0.68	0.17	0.06	z			
	23.0	(17.5)	0.67	0.23	0.01	y			
	40.2	(41.0)	0.23	0.44	0.07	xyz			
	42.4		0.20	0.43	0.15	xyz			
	53.9	(53.2)	0.38	0.58	0.02	xy			
	54.2	(54.0)	0.41	0.53	0.01	xy			
	57.6	(58.1)	0.66	0.34	0.0	xy			
	64.4	(65.6)	0.61	0.31	0.02	xy			
	67.1 ^a		0.00	0.00	0.01	xyz			

^aThis mode is localized on a bond between the fourth and fifth layers.

and N_1 modes in the MD results is caused by the special sampling of the SBZ, which overweights the coupling of these modes to the π and π^* surface states at \bar{J} . The DF-LRT calculations show in particular that, due to the large dispersion of the electronic surface states in the direction of $\bar{\Gamma}\bar{J}$,⁴ the frequencies of the modes N_1 and D (and to a smaller extent also that of D_2) are rather sensitive to the SBZ sampling.

Table I also shows that the frequencies of the N_1 and RW modes at \bar{J} , as well as their splitting, are larger than observed.¹⁰ A number of tests indicate that these values (in particular the RW frequency) should decrease with higher values of E_{cut} , whereas test calculations with a smaller buckling, $b = 0.25$ Å, did not show a significant reduction of the RW - N_1 splitting, contrary to what was suggested by the results of Refs. 8 and 9.

Several features of our results are similar to those of previous semi-empirical calculations.^{8,9} In particular, besides the D and D_2 modes considered above, our calculations confirm the occurrence of the following modes at $\bar{\Gamma}$: (i) two modes above the bulk continuum, at ~ 65 and ~ 68 meV, the former being strongly localized and mostly y polarized (the latter, although mostly localized on a bond between the fourth and fifth layer, is not found to depend significantly on boundary conditions); (ii) a

few yz -polarized modes with frequencies of the order of 50 meV (denoted I' , I'' , and I''' in Table I), which correspond to the “interface” modes discussed in detail in Ref. 9; (iii) a z -polarized “rocking” mode R of rather low frequency (our result, ~ 19.6 meV, is slightly lower than found previously.^{8,9})

The last three columns in Table I show the components of the macroscopic dipole moment $P_{\alpha}^{(n)} = \sum_i \sum_{\beta} (Z_T^*)_{\alpha\beta,i} u_{\beta,i}^{(n)}$ of each mode. Here, $\{u_i^{(n)}\}$ are the Cartesian displacements of the n th normal mode and $(Z_T^*)_{\alpha\beta,i}$ (with $\alpha, \beta = x, y, z$) is the effective transverse (unscreened) charge tensor for the i th atom in the cell. We find that the values of $(Z_T^*)_{xx}$ for the two surface atoms in the 2×1 unit cell are exceptionally large owing to the strong coupling of their x motion to the zone edge π and π^* states, while the other components are at least one order of magnitude smaller.¹⁶ The effective charges are also found to decay quite rapidly into the interior of the slab where $(Z_T^*)_{\alpha\beta} = 0$ is expected on symmetry grounds. As a result, the surface x -polarized modes in the optic region have a much larger dipole moment \mathbf{P} than (y, z) -polarized modes, as it is apparent from Table I. To compare our results with experiments, we computed the dipole-weighted PDOS, $\sigma_{\alpha\alpha} = \sum_n |P_{\alpha,L}^{(n)}|^2 \delta(\omega - \omega_n)$,

where \mathbf{P}_L is the longitudinal (screened) dipole, and compared it directly with the EELS scattering cross section. The screening effect of the substrate is approximately taken into account by dividing the components of the polarization parallel to the surface (i.e., $|P_x^{(n)}|, |P_y^{(n)}|$) by the bulk dielectric constant, $\epsilon_{\text{bulk}} \sim 11.8$.¹⁷ Our results (for m_H equal to its physical value) are shown in Fig. 1: the solid and dashed lines give the computed σ_{xx} and σ_{zz} (the σ_{yy} spectrum is almost zero on the vertical scale of Fig. 1), while the dot-dashed line shows the EELS spectrum taken from Ref. 6. The largest dipole activity comes from vibrations along the surface chains at ~ 57 meV, in agreement with the theoretical results of Ref. 8, and with the experimental data of Ref. 5, where a significant anisotropy of the loss peak is observed. However, at variance with Ref. 8, our calculated σ_{zz} has a non-negligible peak arising from the $(y)z$ -polarized sub-surface modes at $\sim 50 - 55$ meV [the calculated ratio between the zz and xx peak intensities is ~ 0.1 (Ref. 18)]. Therefore our results also provide a consistent explanation of the experimental data of Ref. 6, where an isotropic contribution to the EELS cross section due to modes polarized perpendicular to the surface was found to coexist with the anisotropic contribution of modes polarized along the surface chains.

In conclusion, we have presented a detailed *ab initio* calculation of the phonon spectrum and dipole activity of Si(111)2 \times 1. Our results agree well with the available experimental data, and, in particular, clarify the current controversy on the origin of the observed EELS peak at ~ 56 meV. In addition, they show the important influence

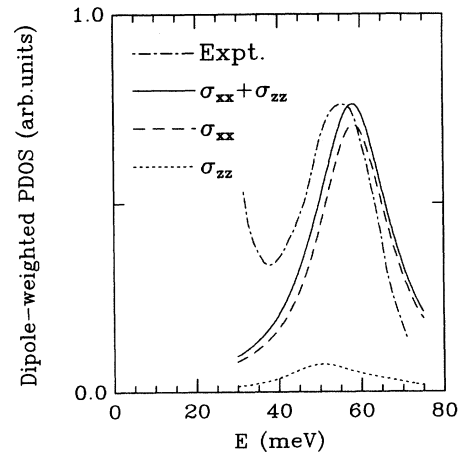


FIG. 1. Comparison between the calculated dipole-weighted PDOS σ_{xx} , σ_{zz} , and their sum $\sigma_{xx} + \sigma_{zz}$ (dashed, dotted, and solid curve, respectively) and the experimental EELS spectrum, Fig.3(a) of Ref. 6 (dot-dashed line). A Lorentzian broadening of FWHM ~ 20 meV has been used to obtain the theoretical curves. The experimental and the theoretical $\sigma_{xx} + \sigma_{zz}$ curves have been normalized to the same height.

of surface localized electronic states on the vibrational properties of this surface.

We thank R. Resta, S. de Gironcoli, P. Giannozzi, and P. Pavone for helpful discussions. This work has been supported by the Italian Consiglio Nazionale delle Ricerche under Grant No. 89.00006.69, and by the European Research Office of the U.S. Army under Grant No. DAJA 45-89-C-0025.

¹For a general review, see, e.g., D.Hanemann, Rep. Progr. Phys. **50**, 1045 (1987).
²K.C. Pandey, Phys. Rev. Lett. **47**, 1913 (1981); **49**, 233 (1982).
³R. Car and M. Parrinello, Phys. Rev. Lett. **55**, 2471 (1985).
⁴F. Ancilotto, W. Andreoni, A. Selloni, R. Car, and M. Parrinello, Phys. Rev. Lett. **65**, 3148 (1990).
⁵N.J. Di Nardo, W.A. Thompson, A.J. Schell-Sorokin, and J.E. Demuth, Phys. Rev. B **32**, 3007 (1986).
⁶U. Del Pennino, M.G. Betti, C. Mariani, S. Nannarone, C.M. Bertoni, I. Abbati, L. Braicovich, and A. Rizzi, Phys. Rev. B **39**, 10380 (1989).
⁷H. Ibach, Phys. Rev. Lett. **27**, 253 (1971).
⁸O.L. Alerhand and E.J. Mele, Phys. Rev. B **37**, 2536 (1988); O.L. Alerhand, D.C. Allan, and E.J. Mele, Phys. Rev. Lett. **55**, 2700 (1985); O.L. Alerhand and E.J. Mele, *ibid.* **59**, 657 (1987).
⁹L. Miglio, P. Santini, P. Ruggerone, and G. Benedek, Phys. Rev. Lett. **62**, 3070 (1989).
¹⁰U. Harten, J.P. Toennies, and C. Woll, Phys. Rev. Lett. **57**, 2947 (1986).
¹¹Stefano Baroni, Pado Giannozzi, and Andrea Testa, Phys. Rev. Lett. **58**, 1861 (1987); P. Giannozzi, S. de Gironcoli, P. Pavone, and S. Baroni (unpublished).

¹²F. Ancilotto, W. Andreoni, A. Selloni, R. Car, and M. Parrinello, Phys. Scr. (to be published).
¹³F.J. Himpsel, P.M. Marcus, R. Tromp, I.P. Batra, M.R. Cook, F. Jona, and H. Liu, Phys. Rev. B **30**, 2257 (1984).
¹⁴D.W. Noid, B.T. Brooks, S.K. Gray, and S.L. Marple, J. Phys. Chem. **92**, 3386 (1988).
¹⁵P. Giannozzi, S. de Gironcoli, and R. Resta, in *Proceedings of the Third International Conference on Phonon Physics*, edited by S. Hunklinger, W. Ludwig, and G. Weiss (World Scientific, Singapore, 1990), p.205.
¹⁶The values of $|P_x|$ in Table I correspond to $(Z_T^*)_{xx} \sim 8.4$ and ~ -7.8 for the "down" and "up" surface atom in the 2 \times 1 unit cell, respectively. These values are affected by some uncertainty, mostly related to the accuracy of the SBZ sampling. However, tests with $E_{\text{cut}} = 6$ Ry suggest that this should not exceed $\sim 30\%$. As a figure of merit, we quote that we satisfy the acoustic sum rule $\sum_i (Z_T^*)_{\alpha\beta,i} = 0$ (which follows from charge neutrality) within $\sim 30 - 50\%$ of a typical Z_T^* value.
¹⁷See, e.g., H. Ibach and D.L. Mills, *Electron Energy Loss Spectroscopy and Surface Vibrations* (Academic, New York, 1982).
¹⁸This ratio becomes ~ 0.2 when m_H is set equal to infinity.